Isotopic study of the influence of oxygen interaction and surface species over different catalysts on the soot removal mechanism

Marina Cortés-Reyes, Juan Carlos Martínez-Munuera, Concepción Herrera, M. Ángeles Larrubia, Luis J. Alemany, Avelina García-García

PII: S0920-5861(21)00323-0

DOI: https://doi.org/10.1016/j.cattod.2021.07.015

Reference: CATTOD13441

To appear in: *Catalysis Today*

Received date: 1 February 2021
Revised date: 30 June 2021
Accepted date: 9 July 2021

Please cite this article as: Marina Cortés-Reyes, Juan Carlos Martínez-Munuera, Concepción Herrera, M. Ángeles Larrubia, Luis J. Alemany and Avelina García-García, Isotopic study of the influence of oxygen interaction and surface species over different catalysts on the soot removal mechanism, *Catalysis Today,* (2021) doi:https://doi.org/10.1016/j.cattod.2021.07.015

Isotopic study of the influence of oxygen interaction and surface species over different catalysts on the soot removal mechanism

Marina Cortés-Reyes[a], Juan Carlos Martínez-Munuera[b], Concepción Herrera[a], M. Ángeles Larrubia[a], Luis J. Alemany[a,*], Avelina García-García[b,*]

[a]*Departamento de Ingeniería Química, Facultad de Ciencias, Campus de Teatinos, Universidad de Málaga, Málaga, E-29071, Spain*

[b]*MCMA Group, Department of Inorganic Chemistry and Institute of Materials, University of Alicante, Carretera de Sant Vicent del Raspeig, s/n, 03690, Sant Vicent del Raspeig, Alicante, Spain*

**Corresponding author.*

e-mail address: luijo@uma.es (L.J. Alemany); a.garcia@ua.es (A. García-García)

Abstract

In order to improve the catalytic formulations for soot removal in after-treatment emission control technologies for gasoline and diesel engine vehicle, an isotopic study was approached using transitory labeled oxygen response method over model catalysts that allows the unraveling of soot oxidation mechanism. Ce-based materials promote oxygen exchange associated with the high population of lattice oxygen species (O^{2-}) denoted as O_I type. The incorporation of praseodymium produces a Pr^{3+} enrichment that decrease the energy for oxygen release and increase oxygen mobility through surface and subsurface oxygen centers (O_{II} type) depending on the synthesis procedure. For PtBaK catalyst, O_{III} species are responsible for oxygen exchange. Gas-solid reaction between soot and gas phase molecular oxygen is responsible for direct uncatalyzed soot oxidation. For ceria containing catalysts, low-temperature soot removal takes place through the intervention of lattice atomic species and superoxide species. For DPNR model catalyst, PtBaK/Al_2O_3, the soot elimination occurs with the intervention O_{III} type centers. In the presence NO, the assisted and cooperative mechanism due to NO_2 and the intervention of the adsorbed nitrate species on the trimetallic catalyst enhances soot removal capacity.

Graphical abstract

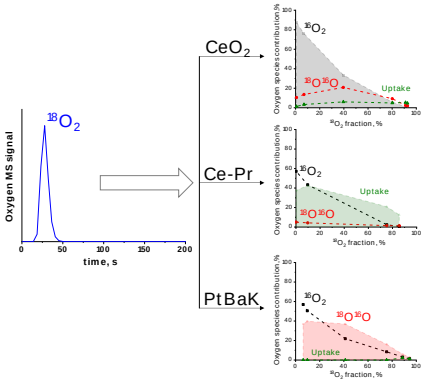

Keywords: soot removal, mechanism, oxygen surface species, isotopic study

1. Introduction

The transportation sector is undergoing a significant transformation, with technologies being rapidly adopted to meet the societal needs of reducing both criteria pollutants - primarily NO_x and particulates – and greenhouse gas (GHG) emissions. Electrification is cited as a panacea but given that more than 97% of new passenger vehicles sold in 2019 were equipped with internal combustion engines, it is imperative to continue improving tailpipe emissions to address health, air quality and global warming concerns [1]. In response to the stringent CO_2 regulations across the major markets, Original Equipment Manufacturers (OEMs) are adopting combined strategies of rapidly advancing IC engine technologies. The situation in Europe is challenging because of the rapid decline in the market share for light-duty diesel, which still provides a 15-20% advantage over gasoline vehicles [2]. However, new recent studies show that improved engine and after-treatment technologies are demonstrating excellent performance, with tailpipe emissions of newly certified diesel vehicles meeting NO_x requirements, even under challenging urban drive conditions [3–5]. In this context, even though Diesel Particulate filter is a mature technology, incremental improvements in their performance are still very valuable to meet overall emission and GHG reduction targets. Therefore, new and optimized soot oxidation catalysts are still needed for enhanced and faster regeneration in streams with lower and lower NO_x percentages due to improved engine technology. Some OEMs are paying attention to new catalysts formulations in an attempt to modify the strategy of using conventional precious metals-formulations as catalysts over DPFs. These are based on the needs to generate large

amounts of NO_2 in order to increase particulate matter oxidation rate, but there are limits to this, since NO_2 reacts with PM yielding NO and it is a challenge to achieve a balance with NOx emission volume. Therefore, attention is now focused on catalysts that are capable of soot oxidation through catalytic reactions using O_2 [6].

Concurrently, gasoline engines, which are gaining market share, are also improving, and recent studies also prove the possibility of 20-30% fuel efficiency gains ahead, with no or mild electrification. In this sense, Gasoline direct injection (GDI) engines have gained popularity in recent years due to the fuel efficiency and performance improvements they offer over Port fuel injection (PFI) engines. GDI vehicles have captured nearly 50% of the market share in USA up to 2016 [7] and boosted, downsized GDI engines offer improved fuel economy over much of the engine map versus traditional gasoline engines [8]. Nevertheless, GDI engines also have some drawbacks compared to PFI engines, such as the superior particulate formation, mainly fine particles (broadly in the 10-100 nm size range). While the emissions may be low on a mass basis, these can be very high (10^{11}-10^{13} #/km) on a number basis. These numbers of particles emitted per kilometer are more than an order of magnitude higher than for PFI engines, exceeding the tailpipe limit of $6 \cdot 10^{11}$ #/km in Europe and China. The ambient ultrafine particulate matter concentrations have a major impact on human health with an increase in all-cause, cardiovascular and respiratory mortality (along several ranges) [9]. Therefore, GPFs have been commercialized and are rapidly becoming a ubiquitous part of new GDI after-treatment systems in Europe and China [1].

A key aspect of the particulate filter operation is the regeneration through the oxidation of the accumulated soot [7]. In diesel applications, passive soot oxidation occurs at appreciable rates by oxidizing soot with NO_2 present in the exhaust gas at temperatures in the range of 300–450 °C, which can be achieved under some medium load conditions. Conversely, in gasoline applications, the exhaust gas temperatures are typically higher compared to diesel. However, due to the high efficiency of the upstream or integrated three-way catalyst (TWC), essentially no NO_2 is available for the passive soot oxidation known from diesel applications. In addition, in normal stoichiometric λ=1 operation, there also is no appreciable oxygen available as oxidant. Oxygen is available only during fuel cuts events, such as decelerations, along with the

required temperatures to oxidize accumulated soot [7,10]. In other words, more or less frequent short fuel cuts motivated by different modes of operation (city or highway driving) lead to transient oxygen concentration which means the occurrence of very short O_2 pulses separated by (free-oxygen) atmosphere periods. In this context, Pt-based catalysts are expensive and quite ineffective for soot combustion in the absence of NO_x. The ability of ceria-based materials to promote oxygen storage/redox behavior is behind their application as practical soot oxidation catalyst under O_2 [11,12]. Therefore, catalysts which could assist soot oxidation under highly transient conditions (long periods with no O_2 supply if the upstream TWC works under stoichiometric conditions) will be demanded. This means that catalysts that lose their surface/subsurface and bulk oxygen very easily creating a sufficient "active oxygen" supply (generating a large population of oxygen vacancies) and, concurrently, with fast kinetics of vacancies reoxidation during the very short oxygen pulses will be the materials potentially suitable for these special and hard working conditions of cGPF [13,14].

In a previous work of some of the authors [15], it was reported that the praseodymium incorporation onto the ceria enhanced the oxygen mobility in the surface/bulk of the sample favouring higher O_2 released amounts under inert atmosphere with regard to ceria. The efficiency of the own active oxygen species released from the catalyst to oxidize soot under inert atmosphere, even under *loose contact* mode, was well demonstrated. In a singular way, at high temperatures under *loose contact* mode, soot could act as a "driving force" and the "own lattice oxygen" could be transferred directly towards soot surface in an efficient way. Based on these premises, Pr-doped cerias can constitute interesting materials to be tested as catalysts in the special conditions demanded by cGPF applications. In these sense, together with Ag-perovskites [16], Ag promoted Fe_2O_3@CeO_2 [13] and Co_3O_4-CeO_2 [14] can constitute other competitive formulations in the new generation of oxygen deliverers catalysts for coating GPFs that operate on GDI engines. Thus, the understanding of the relationship between the catalysts, their oxygen interaction ability and their catalytic activity in the soot removal process under atmospheres with different oxidant nature is required. In order to compare the nature of the different oxygen species present on the catalysts, the labelling indicated by other authors in solids based on perovskites and ceria will be used [17–20] Hence, O_I, O_{II} and O_{III} oxygen type species represent lattice

oxygen species (O^{2-}), surface oxygen species (O_2^{2-} or O^-, O_2^-) and oxygen from surface-chemisorbed groups (OH^-, CO_3^{2-}), respectively.

As far as the authors are concerned, the study of particulate matter elimination through labeled oxygen pulses has not been addressed for cGPF systems and their comparison with other model catalysts should help to improve the catalytic formulations depending on oxygen species and their activity. Therefore, this contribution is focused on the isotopic study of the soot removal mechanism under several oxidant atmospheres when the soot particles are in contact with four representative catalysts for gasoline and diesel engine vehicles, such as pure ceria, ceria-praseodymia mixed oxides and PtBaK catalyst, and the association with their O_2-interaction ability.

2. Material and Methods

2.1. Materials preparation

Model DPNR (Diesel Particulate NO_x Reduction), Pt-Ba-K/γ-Al_2O_3 catalyst, with 118 $m^2 \cdot g^{-1}$, was prepared by wetness impregnation of the support with the precursors to obtain 1.9, 11.5 and 1.4 wt.% of Pt, Ba and K, respectively. The detailed procedure can be found in previous works [21,22]. Model CeO_2 catalyst (57 $m^2 \cdot g^{-1}$) was synthesized by precipitation of $Ce(NO_3)_3 \cdot 6H_2O$ under alkali media. Ceria-praseodymia mixed oxides with $Ce_{0.2}Pr_{0.8}O_2$ composition were prepared following two methods, co-precipitation and direct calcination, as was explained in [15], and the samples, with 10 and 31 $m^2 \cdot g^{-1}$, were labeled as CePr-CP and CePr-DC, respectively. Mixtures between real soot and catalyst (1:9 weight ratio) were prepared by the so-called tight contact method [23], including the mixture with SiC as bare-soot. Real soot was obtained in a motor bench after the use of fuels from different sources in accumulated operation cycles. Its composition in weight consisted of 97%C, 0.7%H, 1.9%O, 0.2%N and 0.2%S, obtained by elemental analysis.

2.2.Experiments with labeled oxygen

The experiments were carried out in a tubular fixed-bed reactor (5 mm of inner diameter) using 280 mg of sample, which consisted of 180 mg of SiC and 100 mg of either catalyst, soot+catalyst or soot, diluted in SiC, keeping the amount of catalyst or soot in the comparative experiments. A continuous flow of 8 ml·min^{-1} of He or 10,000 ppm of NO in He was used as a carrier, and the temperature was modified from 300 to 750ºC (in steps of 50ºC). At each temperature, two pulses of $2.5 \cdot 10^{-6}$ mol of $^{18}O_2$ were introduced through an injection valve with a 100 µl loop, which was previously evacuated with a vacuum pump and filled up with the isotopic gas at 9 psi, and then, the product distribution was analyzed by mass spectrometry using an OmniStar model from Pfeiffer Vacuum. The compounds that were mainly analyzed and their corresponding m/z lines are: $C^{16}O/N_2$ (28), $C^{18}O/NO$ (30), $N^{18}O/^{16}O_2$ (32), $^{18}O^{16}O$ (34), $^{18}O_2$ (36), $C^{16}O_2$ (44), $C^{18}O^{16}O/N^{16}O_2$ (46), $C^{18}O_2/N^{18}O^{16}O$ (48), $N^{18}O_2$ (50). For the coincident lines, the distribution has been estimated through the secondary lines.

3. Results and Discussion

3.1. Pulses of $^{18}O_2$ over the catalysts

In order to analyse first the nature and degree of interaction between gas phase $^{18}O_2$ and the surface of every catalyst four representative/potential fresh catalysts of engine emission control technologies were chosen. Pulses of $^{18}O_2$ were injected under He as carrier at several temperatures (from 300-750°C). Average values of two pulse experiments at a given temperature were taken for the evaluation of the response of the catalysts.

It is important to outline that a preconditioning treatment under helium was carried out for comparative purposes. This latter treatment led to obtain experimental data which would preclude the correct comparison between the results obtained from bare catalysts with those obtained with the soot/catalysts mixtures but allowed the oxygen mobility to be analyzed in depth. Taking these premises into account, the catalysts were only submitted to a heating ramp under helium stream from room temperature to the first reaction temperature (300°C), in order to stabilise temperature and MS signals for the data represented in Fig. 1 a-d. The absence of a pre-conditioning step under $^{16}O_2$ can

complicate the interpretation of the experimental data. However, the discussion will be conducted on the basis of qualitative differences on catalysts' behaviours in terms of interaction and oxygen uptake as well as the oxygen isotopologues species release considering a same procedure.

Figure 1.a-d displays the percentages of oxygen isotopologues in the gas phase associated with the pulse at the outlet of the reactor measured at the different temperatures. These values were calculated by comparing the sum of the obtained data of every oxygen species with the $^{18}O_2$ whole area of the isotopic pulse, conducted at every temperature, with the reactor loaded with SiC as inert. Different profiles are seen comparing the four catalysts selected, indicating the relevant influence of the chemical nature of the catalyst on its interaction with oxygen. Nevertheless, all of them are characterized by a common feature: as soon as the $^{18}O_2$ pulse is fed to the reactor, its level decreases significantly from the starting temperature. Considering firstly the PtBaK catalyst (Fig. 1d), the decrease in the isotope percentage of $^{18}O_2$ with increasing temperature is balanced by increases of the $^{18}O^{16}O$ species (the predominant isotopologue up to 500°C with around 40% of contribution) and $^{16}O_2$, therefore, no significant oxygen uptake is registered along the whole experiment as indicated by the green line, and, exclusively, oxygen isotopic exchange is taking place for the Pt catalyst.

The basic theory of isotopic exchange considers two kinetically resolvable types of isotopic exchange, (excluding the zero-atom exchange which takes place at very low temperatures), [24,25], namely:

i) single-atom exchange between one oxygen atom from the gas phase oxygen molecule and one oxygen atom from the solid. It involves surface (or subsurface atoms of the solid), Os, and may be presented as follows:

$$^{18}O_2 + {}^{16}O_S \leftrightarrow {}^{18}O^{16}O + {}^{18}O_S \quad (1)$$

$$^{18}O^{16}O + {}^{16}O_S \leftrightarrow {}^{16}O_2 + {}^{18}O_S \quad (2)$$

ii) two-atom exchange between molecule O_2 and two oxygen atoms from the solid:

$$^{18}O_2 + 2{}^{16}O_S \leftrightarrow {}^{16}O_2 + 2{}^{18}O_S \quad (3)$$

$$^{18}O^{16}O + 2^{16}O_S \leftrightarrow {}^{16}O_2 + {}^{18}O_S + {}^{16}O_S \quad (4)$$

$$^{18}O^{16}O + 2^{18}O_S \leftrightarrow {}^{18}O_2 + {}^{18}O_S + {}^{16}O_S \quad (5)$$

Since the predominant product for the PtBaK catalyst is $^{18}O^{16}O$, the isotopic exchange seems to proceed (at least at low temperatures) by a single atom-exchange type. This supported catalyst over a non-reducible oxide, as Al_2O_3, was prepared according to a monolayer coverage [21] and the accessible surface oxygen was minimum and O_{III} type [17], characteristic of hydroxyls, alkaline oxide and even carbonate species present in this material [21,26] as can be observed in the XRD diffractogram (Fig. S1), which has a lower nucleophilicity than O_I type species [27].

The profiles exhibited by Ce-containing catalysts are quite different compared with that of Pt and among each other as well. Therefore, all these different behaviors can be considered as a *fingerprint* for the relative rate of oxygen incorporation versus oxygen dissociation and evolution or products [28]. For the bare ceria catalyst, a minor O_2 uptake percentage can be measured from the beginning of the experiment up to 550°C. From 300 to 550°C, some types of interactions among the $^{18}O_2$ pulse and the *in situ* vacancies created (during the heat treatment for temperature stabilization) could happen, as well as interactions with other surface groups, which could explain the low percentages of oxygen uptake. From 550°C, only isotopic exchange is registered with relevant predominance of $^{16}O_2$ product, in agreement with the results published by *Sadovskaya et al* [25], where the authors reported that two-atom exchange most often occurs in transition metal oxides widely used in heterogeneous oxidative catalysis.

A notable feature seen from Figure 1a (the ceria catalyst) is the occurrence of a maximum in the temperature dependence of the $^{18}O^{16}O$ isotopic species (this feature was also reported for other mixed oxides) [28–30]. This observation can be tentatively accounted for the two-scheme single atom exchange [29]. As more and more $^{18}O^{16}O$ evolves, this interacts with the catalyst's oxygen, yielding $^{16}O_2$, since immediately after the appearance of the maximum, $^{16}O_2$ level also increases. Whatever the reaction temperature tested, the $^{16}O_2/^{18}O^{16}O$ ratio remains very high, with values close to 6 at 500ºC, suggesting that the predominant mechanism is the two-atom exchange as usual in transition metal oxides, therefore, the fact that the rate of oxygen incorporation is higher than that of oxygen dissociation could be inferred here [28].

Concerning mixed oxides, CePr-CP, but specially CePr-DC, interact with $^{18}O_2$ isotopic in an effective way, the exchange kinetics with the isotopic pulse is faster, and the consumption of the pulse is already complete at 450°C for CePr-DC. For these two catalysts, which are characterized by a same Ce/Pr composition, a single cubic fluorite-type structure was detected, (similar to that of ceria's catalyst, see Fig. S1 and corresponding description in SI for additional details), but different BET surface areas, crystallinity and Pr^{3+} content (because they were synthesized by different methods) were reported [15]. The profiles of both mixed oxides (Fig. 1b,c) are clearly different if compared with those of pure ceria (Fig.1a) since relevant oxygen uptake is monitored along the experiments. This large capability of the ceria-praseodymia mixed oxides to incorporate oxygen can be partially explained by their ability to evolve oxygen, even under inert atmosphere (Fig. S2). This Figure evidences the relevant differences, in terms of ability to release oxygen, motivated by the incorporation of Pr into the ceria lattice. PtBaK and CeO_2 do not exhibit capability to release oxygen under inert atmosphere whereas the amount of oxygen released by CePr-CP and CePr-DC was 735 and 745 μmol $O_2 \cdot g_{cat}^{-1}$, respectively, being 22.7 and 7.4 the number of monolayers affected by the catalysts' reduction originated by their corresponding oxygen release. Therefore, not only the catalysts' surface is involved but also a considerable and different number of sub-surface and bulk layers are involved in the oxygen diffusion process for these two catalysts. It is supposed that the "fresh" oxygen vacancies (being eventually a remarkable population for these two mixed oxides) created during the step of heating under helium and/or during the increase of temperature (from 300 to 750°C) along the whole experiment, can act as "trap" for oxygen uptake, due to the relevant percentage of oxygen incorporation. At low temperatures, the predominant response of these two catalysts is the oxygen uptake. There was a simultaneous evolution of $^{16}O_2$ and $^{18}O^{16}O$, being the former the main oxygen species with a maximum at intermediate temperature, but the profiles are different from those of the ceria catalyst and the $^{16}O_2/^{18}O^{16}O$ ratio values were higher, around 10 for CePr-DC at 500ºC. This observation can be due to a certain contribution of the $^{16}O_2$ release from the catalyst (the profiles exhibited on Figure S2 indicate a large oxygen release capacity for Pr-containing catalysts) [15]. As $^{18}O_2$ is uptaken, even though $^{16}O_2$ keeps being the prevalent species, both $^{16}O_2$ and $^{18}O^{16}O$ levels tend to similar contributions at high temperatures. Therefore, for these catalysts, the interaction with oxygen is dominated by

the incorporation of the $^{18}O_2$ pulse and the evolution of products is conditioned by the level of oxygen uptake.

In an attempt to confirm the validity and interest of these results, when the experiments were conducted with a previous preconditioning treatment at 500°C under He (for 1 hour), excluding the percentages of oxygen uptake, (which seem to be very sensitive to the previous thermal history of the catalyst), the results (Fig. 1 e-h) seem to be relatively similar for the case of Pt and ceria-catalyst (which are characterized by lower abundance and mobility of oxygen species and the $^{16}O_2/^{16}O^{18}O$ ratios kept below 1 at temperatures lower than 500ºC). On the contrary, the profiles are different from CePr catalysts that exhibited $^{16}O_2/^{16}O^{18}O$ ratios around 3 for the same temperature range, which are lower than those observed in the absence of the pre-treatment. This could be explained by the fact that more highly reactive $^{16}O_2$ species are evolved during the previous thermal treatment up to 500°C (and the subsequent stepwise experiment) than those with only a pre-treatment at 300°C. In agreement with information compiled in Figure S2, $^{16}O_2$ species for Ce-Pr catalysts can suffer some degree of "exhaustion" in their populations, which obviously causes the ratios to decrease. This provides some insight into the different origins of $^{16}O_2$ (depending on the catalysts' nature) from a mechanistic point of view. In some way, the abundance and mobility of labile species of oxygen on Ce-Pr catalysts influence on the evolution of their isotopologues.

Therefore, the differences between these materials are oxygen type, their chemical environment and abundance of oxygen vacancies at the beginning of the stepwise pulse isotopic experiment, which can influence their activity towards O_2. Ce-based materials promote different degrees of oxygen uptake and activity towards oxygen exchange. A notable population of oxygen vacancies created during the different pre-treatments favors the decrease in $^{16}O_2$ level (because of O_{II} (O_2^{2-}, O_2^- type species) depletion), which is clearly manifested in Ce-Pr mixed oxides. The incorporation of praseodymium to CeO_2 structure involves activation of surface and subsurface oxygen centers [15], increasing oxygen release capacities and further oxygen uptakes through vacancies created on previous O_{II} type species together with lattice oxygen species, due to fast sub-surface and bulk oxygen diffusion (as supported by Figure S2). Conversely, for PtBaK catalyst, less electron-rich O_{III} species are able to exchange oxygen according the general steps of isotopic exchange and maintain oxygen balance without registering any uptake whatever the conditions used.

3.2. Soot removal

To delve into the mechanism of soot elimination and the relationship with the interaction of the catalysts with oxygen, experiments of $^{18}O_2$ pulses at different temperatures have been carried out on catalyst samples with soot under helium atmosphere. In Figure 2, the fraction of $^{18}O_2$ detected during a pulse at the outlet is presented with respect to the amount of labeled oxygen fed as a function of temperature, as an intuitive way of expressing labeled oxygen consumption. Although in all cases a decrease in the amount detected is observed as the temperature increases, the slope, which would be associated with the rate of oxygen consumption in the gas phase, and the amount consumed are different depending on the system used. It should be noted that $^{18}O_2$ consumption may be due to the combination of oxygen uptake and exchange with the oxygen coming from the material, and the soot removal process, the latter being more relevant.

In the absence of a catalyst, considerable oxygen consumption occurs in the range between 500 and 700°C, which should be due to the interaction between carbon and oxygen in the gas phase, requiring high temperature for the process to take place. This temperature range is similar to that observed by other authors who have studied the non-catalytic removal of soot [31]. The temperature at which 50% of inlet oxygen was consumed was found around 550ºC, similar to T_{50} value estimated for soot removal in the absence of catalyst under oxygen atmosphere [32,33] and characteristic of real soot elimination, which is lower than the value shown by the model soot [31]. For the catalyst + soot mixtures, even at low temperature, $^{18}O_2$ consumption is observed that could be due to the exchange or oxygen uptake (explained in the previous section) or by reaction with carbon. The PtBaK catalyst, which is characterized by less oxygen uptake and exchange capacity, requires higher temperatures to achieve similar levels of oxygen consumption than Ce-based materials, indicating less activity in the soot removal process, as was expected. The catalysts based on ceria are the most active in oxygen consumption, without detecting the oxygen fed at the outlet when the temperature is higher than 500ºC. While the temperature at which 50% of fed oxygen is consumed was 410ºC for PtBaK, for Ce-containing catalysts that value was below 400ºC; however, the preparative of the catalyst has an influence because it is above and below than bare CeO_2, depending on the synthesis procedure that conditions surface area, crystallinity

and species distribution. The decrease in soot removal temperature for Ce-based materials compared to PtBaK catalysts is in consonance with the data estimated in a previous work with the use of model Printex U soot [23], confirming the possibility of using this model soot to represent the behavior of real soot and the higher oxygen interaction capacity of mixed oxides respect to supported PtBaK catalysts.

In order to better understand the soot removal mechanism, labeled product distribution has been further analyzed. Although low amounts of CO isotopologues were detected, CO_2 was the main species. In the absence of catalyst, the evolution of CO_2 isotopic molecules during a $^{18}O_2$ pulse at different temperatures is displayed in Figure 3. Quasi-symmetric signals of $C^{18}O_2$, $C^{18}O^{16}O$ and $C^{16}O_2$ were registered whose maxima values were reached around 22 s, with peak widths at half height close to 12s. In addition, $C^{18}O^{16}O$ and $C^{16}O_2$ intensities were between 1 and 2 magnitude orders lower than the values obtained for $C^{18}O_2$, the latter being the main species and considering the amounts of other isotopic molecules to be negligible. This trend was proven by a semi-quantitative analysis of the signals through the integration of MS signal intensities along the pulse time (Fig. S3), where the highest contribution of $C^{18}O_2$ was also confirmed. This implies that the species that are responsible for CO_2 formation were invariably the same and, consequently, there is a single soot elimination process through the interaction of carbon and gas phase by a gas-solid reaction. As can be observed (Figs. 3 and S3), as temperature increased the signals associated with CO_2 and the activity of the process also increased up to 600ºC. From this temperature, the intensities were maintained and coincided with the temperature interval in which the consumption of the fed oxygen was complete, as was seen in Figure 2, indicating that this process is favored at high temperatures.

Then, the mechanism of uncatalyzed soot removal occurs via intervention of gas phase oxygen [22,23,34], as indicated in the following equation:

$$(C - C^*)_n\ (s) + {}^{18}O_2\ (g) \rightarrow C^{18}O_2\ (g) + (C - C^*)_{n-1}\ (s) \qquad (6)$$

where C* is an accessible carbon center of the carbon chain to be oxidized that interacts with the labeled oxygen molecule producing $C^{18}O_2$, as was observed in Fig. 3, and yields the decrease of the soot carbon chain. The intervention of the oxygen contained in particulate matter was discarded due to the product distribution, but the incomplete combustion with CO formation is a co-side reaction that took place in a low proportion [35], according to the reaction:

$$(C - C^*)_n\ (s) + {}^{18}O_2\ (g) \rightarrow 2C^{18}O\ (g) + (C - C^*)_{n-2}\ (s) \qquad (7)$$

In the presence of whatever catalyst tested, the trend of the isotopic product distribution was completely different, even though CO_2 was also the main product versus CO. For the catalyzed soot removal, CO_2 isotopic distribution after the feeding of $^{18}O_2$ pulse is represented in Figures 4 and 5 for the experiments carried out at 350 and 500ºC, respectively. At 350ºC (Fig. 4), contrary to bare soot profiles, $C^{18}O_2$ intensity was two orders of magnitude lower than $C^{16}O_2$, independently of the catalytic formulation, being in the limit of the analyzer detection and probably caused by a signal perturbation of other signals; besides, $C^{18}O^{16}O$ signal intensity was one decade lower and was not representative either. Thus, the main CO_2 isotopologue detected was $C^{16}O_2$, which indicated the intervention of oxygen species different from gas phase molecular oxygen. Furthermore, while the non-catalytic CO_2 signals were symmetric, the profiles for the catalyzed process presented a pronounced tail and the height and width depended on the catalyst formulation, indicating that there was more than one type of species involved in the formation of CO_2. At low temperatures, trimetallic catalyst consumed less oxygen that those based on ceria (Fig. 2), which is due to the lower oxygen interaction and uptake capacity detailed in the previous section, the lower activity in soot removal process or the combination of both factors. The lowest CO_2 production detected for PtBaK catalyst (Fig. 4) compared to those of CeO_2 indicates that higher temperatures should be reached to obtain similar soot conversion values, due to different oxygen species are involved in the removal process. In a previous work [23] the better activity of Ce-containing catalysts compared with that of PtBaK was also observed and can be related to the fact that the trimetallic catalyst is less efficient in the "active oxygen"-assisted soot combustion reaction, associated with its lower oxygen activation capacity (uptake and exchange) explained in Figure 1. Although noble metals can improve soot oxidation capacity of CeO_2 when this latter is used as a support [36] since this incorporation enhance the ability to generate oxygen vacancies, oxygen species in bulk CeO_2 make oxygen mobility easier than that typical of O_{III} species of the trimetallic catalyst supported on Al_2O_3.

On the other hand, the incorporation of praseodymium to CeO_2 structure increased the width of the CO_2 peak and the time where CO_2 emission, as a long tail, takes place. As can be observed in the inset, where normalized signals for Ce-containing catalysts were shown, the formation of CO_2 during the inert period was higher due to

the fact that Ce-Pr mixed oxides are characterized by higher oxygen mobility in the subsurface/bulk of the catalysts [15], being the energy required to release oxygen lower than that of CeO_2 [37] and, consequently, makes its application in gasoline particle filters possible by increasing the release of oxygen during the long inert periods, after oxygen pulses, typical of the real working conditions of these efficient engines (Figs. 1 and S2). The synthesis procedure influenced the crystallinity, the surface area value as well as the Pr^{3+} surface content, obtaining higher values for the samples prepared by direct calcination (31 vs 10 $m^2 \cdot g^{-1}$ and 45 vs 31% of Pr^{3+}) [15]. Those parameters influence the oxygen uptake capacity and the oxygen exchange, being more active when the direct calcination of the metallic precursors was used, since more pathways for fast chemical diffusion can be created [38], involving Pr species, that promote oxygen mobility and assist the elimination of soot.

Although the formation of CO_2 is kinetically dependent on the catalyst's formulation, all cerium-containing catalysts follow the same mechanism that could be sequential through surface oxygen species both from vacancies and those created by defective surface oxygens (O_I and O_{II}), whose proportion depended on the synthesis procedure and composition and make the removal of soot effective at low temperatures. It is generally accepted that soot oxidation over CeO_2-based catalysts occurs through a Mars-van-Krevelen mechanism [23,39] but, taking the obtained profiles into account, can be expressed as follows.

$$(C - C^*)_n\,(s) + 2Ce(Pr)^{16}O_2\,(s) + {}^{18}O_2\,(g) \rightarrow C^{16}O_2\,(g) + 2Ce(Pr)^{16/18}O_x\,(s) + (C - C^*)_{n-1}\,(s) \quad (8)$$

$$(C - C^*)_{n-1}\,(s) + 2Ce(Pr)^{16/18}O_x\,(s) + {}^{18}O_2\,(g) \rightarrow C^{16}O_2\,(g) + 2Ce(Pr)^{18}O_2\,(s) + (C - C^*)_{n-2}\,(s) \quad (9)$$

The decrease in the length of the carbon chain is promoted by the generation of oxygen vacancies on the catalysts, which transfer into O_x^- [12,14], and these species can spill over onto soot particles in order to completely oxidized them, being regenerated by gaseous oxygen or by catalyst sub-surface/bulk oxygen. The formation of oxygen vacancies and the higher rate of creation of active oxygen species are enhanced by the presence of praseodymium in the formulation, being more noticeable in the case of the best physicochemical features present on the catalyst obtained with the direct calcination method (higher BET surface area and Pr^{3+} enrichment on catalyst's surface), which is characterized by the same mechanism with a higher oxygen release and O_x^-

transfer onto the surface. This mechanism is consistent with the highest $C^{16}O_2$ formation, followed by $C^{18}O^{16}O$ and being the formation of $C^{18}O_2$ almost negligible.

As temperature becomes higher, several differences were noticed in the distribution of CO_2 isotopologues. At 500ºC (Fig. 5), the intensity of all the signals considerable increased and CO_2 production time duration was decreased, more discernible for Pr-containing catalysts, which presented the highest values before. This observation was associated with a higher consumption rate of soot with temperature. Although $C^{16}O_2$ was still the main product and its production was higher for Ce-based catalysts, the proportion of the scramble $C^{18}O^{16}O$ considerably increased, and that increment was more notable for PtBaK, which had less surface oxygen available. The main mechanism followed by this type of catalysts is summarized in the following reaction.

$$(C - C^*)_n\ (s) + Pt\text{-}^{16}O\text{-}M\ (s) + {}^{18}O_2\ (g) \rightarrow C^{18}O^{16}O\ (g) + Pt\text{-}^{18}O\text{-}M\ (s) + (C - C^*)_{n-1}\ (s) \quad (10)$$

Different from Ce-containing catalysts, in this system the decrease in the carbon chain is associated with the intervention of Pt-O-M centers, where M represents an alkaline or alkaline-earth metal (K or Ba), as was reported before [22]. This oxygen species (O_{III}) related to hydroxyl and carbonate species are less nucleophilic than O^{2-} species, but an active electron can be released through the alkali for the generation of a nucleophilic oxygen species [40,41]. The electron donor character of alkaline and alkaline earth metal oxides produces an increment in the strength of carbon-oxygen bonds and, consequently, the C-C bond is weakened [34,42,43], and the number of carbon atoms decreases, generating CO_2 with at least one unlabeled oxygen.

In order to understand the isotopic distribution according to temperature, the area integration of each CO_2 isotopologue MS intensity with the pulse time was carried out and the results obtained for the four catalysts are represented in Figure 6. The intensity of $C^{16}O_2$ isotopic species increased with temperature up to its stabilization at temperatures higher than 500ºC. For $C^{16}O^{18}O$ signal, an increasing linear trend was observed in the low temperature range, whereas for the PtBaK catalyst the intensities increased and were stabilized. A sigmoidal trend was observed for $C^{18}O_2$ signal, with higher intensities as temperature increases due to the intervention of oxygen in the gas phase. It should be noted that for the PtBaK catalyst the contribution is notable at lower temperatures than for Ce-based catalysts due to its lower oxygen release and oxygen exchange capacity. These data confirm that soot combustion under inert atmosphere and

tight contact conditions proceeds by oxygen emitted from the catalyst or by the own lattice oxygen (O_I and O_{II} type), justifying higher $C^{16}O_2/C^{16}O^{18}O$ ratios for Ce-containing catalysts compared to PtBaK, acting soot as a "driving force" and being able to extract the available and more reactive surface/sub-surface/bulk oxygen. This is promoted by ceria-praseodymia mixed oxides exhibiting high oxygen mobility, not only at the surface level, but also at sub-surface/bulk level (Fig. S2). The contribution of CO_2 isotopologues during soot combustion and the O_2 isotopic gas phase distribution during the pulse of labeled oxygen in the absence of soot are related. PtBaK catalyst has no lattice oxygen available and there is no oxygen uptake during $^{18}O_2$ pulses, resulting in a high contribution of $^{16}O^{18}O$ and $^{16}O_2/^{16}O^{18}O$ ratios lower than 1, at temperatures lower than 500ºC. This fact results in a poor soot oxidation activity with the lowest $C^{16}O_2/C^{16}O^{18}O$ ratio values in the range of 1-2, depending on the reaction temperature, of all the tested catalysts. Ceria has limited mobility of bulk oxygen, but higher $^{16}O_2/^{16}O^{18}O$ ratios than those for PtBaK catalyst. In fact, $C^{16}O_2/C^{16}O^{18}O$ ratio values were four times higher than the trimetallic catalyst, due to the higher amount of surface oxygen available to assist the removal of soot. Ce-Pr catalysts present much better ability to release oxygen and to incorporate and stabilize a large population of oxygen vacancies, due to better reducibility of Pr cations versus Ce cations, which implies higher $C^{16}O_2/C^{16}O^{18}O$ ratios (close to 10). Nevertheless, the response towards soot combustion between both Ce-Pr samples is very different although the mechanism is identical. The lower activity of CePr –CP catalyst can be explained by its very low surface area that restrict the participation of sub-surface/bulk oxygen in soot the removal due to a lower number of contact points. However, the activity towards soot combustion at low temperatures is more favored for CePr-DC catalyst, since the long tails of CO_2 emissions and the higher $C^{16}O_2$ contribution pointed out the participation of sub-surface layers of oxygen and abundant oxygen species.

Therefore, under helium atmosphere, in the presence of catalyst, real soot removal takes place via two main pathways that involved electron donation to carbon and oxygen transfer to carbon. The former is promoted by PtBaK catalyst through O_{III} oxygen species whereas the latter requires the formation of O_I or O_{II} species characteristic of CeO_2-based materials.

3.3. NO interaction

Nitrogen oxides are present at the outlet of the exhaust pipe of current diesel engines and can be found in some operation conditions of gasoline vehicles, although in low concentration [10]. Therefore, the analysis of the impact of these species in the real soot removal process in the presence of different catalysts is of high interest. For that, pulses of labeled oxygen under 1%NO in helium atmosphere were performed at different temperatures over soot+catalyst mixtures. The percentage of $^{18}O_2$ detected at the outlet respect to the fed oxygen is represented in Figure 7 for bare soot, PtBaK and Ce-based materials. At 400ºC, the concentration of oxygen at the outlet was 6% lower in the presence of NO than under He atmosphere for the uncatalyzed process, indicating that more oxygen was consumed, with a practically linear slope with temperature in the low temperature range. The increase in the oxygen consumption rate was associated with the more oxidizing nature of NO/NO_2 atmosphere. It is generally accepted that NO_2 is a better oxidant than O_2 and shifts soot ignition to lower temperature [44,45]. Although labeled CO_2 is still the main species by reaction between carbon and oxygen in the gas phase, an increase in unlabeled CO_2 contribution was observed compared to He atmosphere. This is due to the shortening of the chain by reaction with the NO or NO_2 in the gas phase, being the latter formed from the low conversion of the NO that is fed [23], through these reactions.

$$2N^{16}O\ (g) + {}^{18}O_2\ (g) \rightarrow 2N^{18}O^{16}O\ (g) \quad (11)$$

$$3N^{16}O\ (g) \rightarrow N^{16}O_2 + N_2{}^{16}O\ (g) \quad (12)$$

Thus, soot removal can occur via the following pathway in which the decrease in the carbon chain is produced by gas phase molecules with formation of labeled species, which takes place at lower temperatures than combustion with only O_2 gas phase, in agreement with the gas-solid reaction in the presence of NO_2 and oxygen [46,47]. In addition, an increase in $N^{18}O$ signal was detected, confirming the occurrence of the following reaction, which confirmed the mechanism already proposed for model soot [22].

$$(C - C^*)_n\ (s) + N^{16}O\ (g) + {}^{18}O_2\ (g) \rightarrow C^{18}O^{16}O\ (g) + N^{18}O\ (g) + (C - C^*)_{n-1}\ (s) \quad (13)$$

In the presence of any catalyst, labeled oxygen consumption was higher than for bare soot. Consumption profiles according to temperature was similar for CeO_2-based materials and at lower temperature range than trimetallic catalyst. For PtBaK, the temperature at which 50% of $^{18}O_2$ is consumed was shifted 25ºC below the inert atmosphere, from 410 to 385ºC. These O_2 consumption values indicated that other

reactions took place in the presence of NO and gas phase oxygen was involved. The CO_2 isotopic distribution obtained during the oxygen pulses for the catalytic soot removal process in the presence of NO are displayed in Figure 8 and were necessary to understand the mechanism of the carbon elimination. For Ce-based materials, the profiles were similar to those observed under inert atmosphere without detecting a considerable increase in CO_2 production, in spite of registering a higher $^{18}O_2$ consumption, being $C^{16}O_2$ the main product. This fact indicated the occurrence of parallel processes that took place, as NO oxidation, but did not contribute to soot removal. In consonance with other authors [44,48], for Ce-containing catalysts + soot mixtures prepared by tight contact method, NO oxidation and nitrate formation could be partially inhibited because soot particles are covering the surface of the catalysts reducing the oxygen balance and, consequently an increase in CO_2 production was not observed. However, for PtBaK catalysts, in addition to the increase in CO_2 formation, the shape of the profile was different with a maximum around 58 s and a shoulder at 23 s, which can be related to the occurrence of two sequential processes. The unlabeled and the scramble CO_2 isotopologues were the main species, whereas the formation of $C^{18}O_2$ can be ruled out. Furthermore, N_2 evolution was also detected simultaneously to CO_2 production, confirming the occurrence via this NO_2-assisted mechanism [22,49,50].

$$(C - C^*)_n\ (s) + 2N^{16}O_2\ (ads) \rightarrow 2C^{16}O_2\ (g) + N_2\ (g) + (C - C^*)_{n-2}\ (s) \qquad (14.1)$$

$$(C - C^*)_n\ (s) + 2N^{18/16}O_2\ (ads) \rightarrow 2C^{18}O^{16}O\ (g) + N_2\ (g) + (C - C^*)_{n-2}\ (s) \qquad (14.2)$$

NO was first oxidized by the catalyst [$N^{16}O$ (g)+ $^{16}O_{-cat} \rightarrow N^{16}O_{2-cat} \rightarrow N^{16}O_2$ (ads)] and/or by the gas phase labeled oxygen [$2N^{16}O$ (g)+ $^{18}O_2$ (g) $\rightarrow 2N^{18/16}O_2$ (g) $\rightarrow 2N^{18/16}O_2$ (ads)] to NO_2, which was stored as nitrate species ($N^{16}O_2$ (ads) and $N^{18/16}O_2$ (ads)) onto the catalyst surface. These species are represented in eq. 14.1 and eq. 14.2 as $N^{18/16}O_2$ (ads) since it was not possible to know with absolute certainty the exact origin of each of the oxygens involved because there was an interaction between labeled oxygen from gas phase and unlabeled oxygen from the catalyst and the inlet NO. On the other hand, the production of unlabeled CO_2 was confirmed and represented as $C^{16}O_2$ and the scramble $C^{18}O^{16}O$ isotopic molecule in eq. 14.1 and eq. 14.2, respectively. This mechanism of elimination of soot suggests the intervention of surface nitrate species involved in the oxidation and shortening of the carbon chain in the presence of NO and oxygen, which is similar to that proposed by other authors in an atmosphere of NO_2 +

O_2 [51–53], in which the cooperative interaction between oxygen and NO_2 through the decomposition of surface oxygen complexes was responsible for the elimination. Nitrate species are responsible for the enhancement in soot elimination process generating active oxygen species [54] and, according to *Matarrese et al* [55], the thermal decomposition of these species was not necessary, only their mobility without the intervention of the noble metal. The catalysts more effective in these sequential reactions are more suitable for their use in the simultaneous removal of NO_x and soot. A priori, the activity in the NO_2 assisted mechanism should be related to NO oxidizing capacity of the material, so it must be analyzed.

In order to study the oxidation of NO in the absence of soot, pulses of labeled oxygen were performed on the catalysts under a NO atmosphere. In figure 9, NO profiles along time for a pulse performed at low temperatures are presented, with an inset of the distribution of the isotopic species of NO_2. NO consumption was detected simultaneously to the feeding of labeled oxygen and was higher for the trimetallic catalyst than for those based on ceria, being considerable during 100 s. This consumption may be due to the oxidation of NO to NO_2 and/or the formation of nitrates. To better understand NO oxidation process, NO_2 isotopologues distribution has to be considered. NO_2 production is higher at lower temperatures due to the exothermic character of the reaction [56]. As was observed, unlabeled $N^{16}O_2$ was the main product, the amount of scramble $N^{18}O^{16}O$ was low and $N^{18}O_2$ was not detected. This indicates that the oxidation takes place through the oxygen of the catalyst (O_{2cat}) through the following reaction [35] without the intervention of gas phase molecular oxygen except to keep catalyst species in an oxidized form.

$$2N^{16}O\ (g) + {}^{16}O_2cat \rightarrow 2N^{16}O_2\ (g) \qquad (15)$$

This process depended on the surface oxygen availability, which has been proven to be higher for cerium oxides than for PtBaK. However, although CeO_2-based materials are able to oxidize NO to NO_2, their activity was lower than for noble metal containing catalysts [49]. In addition, for the trimetallic catalyst, NO consumption was considerably higher than NO_2 production confirming the formation of nitrate species onto the catalyst, that are involved in soot removal. Then, other characteristics different from the oxygen interaction capacity have to play a role in NO oxidation and nitrate formation. Among them, alkaline earth oxides present a stronger basicity compared to CeO_2 favoring the nitrite/nitrate adsorption [57], and well dispersed noble metals are

responsible for NO oxidation [58] and are more active than mixed oxides [59], which are modified or combined to increase the oxidation activity. All these factors make PtBaK/Al_2O_3 a suitable catalyst for Diesel Particulate NOx Reduction (DPNR) technology. The lower oxidation capacity besides the poor interaction of Ce-based catalysts with NO in the presence of soot inhibit the improvement due to NO_2-assisted mechanism.

Therefore, the soot removal process depends on the nature of the catalytic surface, the oxygen interaction capacity and the reaction atmosphere. Ceria-based catalysts showed higher oxygen exchange capacity and reduced the temperature of soot removal via intervention of surface oxygen (O_I and O_{II} species). The presence of praseodymium in the mixed oxide increased the release of lattice oxygen during the inert period. Pt-Ba-K/Al_2O_3 was able to remove particulate matter involving O_{III} type species with alkaline centers. Under more oxidant atmosphere, the temperature of soot removal decreased, and additional routes appeared by interaction of NO gas phase and adsorbed nitrates with the soot sample.

4. Conclusions

An isotopic study over model catalysts representative of after-treatment emission control technologies in gasoline and diesel engine was established for unraveling real soot removal mechanism. By $^{18}O_2$ pulses it has been established that the fraction of each isotopologue detected is related to oxygen surface species and the interaction with the catalyst. In the absence of catalyst, it has been proven that the gas-solid reaction between soot and gas phase molecular oxygen is responsible for direct soot oxidation. For ceria containing catalysts, low-temperature soot removal takes place through the intervention of surface oxygen (O_I and O_{II} type species), both lattice atomic species and superoxide species. For DPNR model catalyst, PtBaK/Al_2O_3, a low oxygen exchange capacity was registered, but the soot elimination occurs with the intervention of hydroxylated groups and oxide centers (O_{III} type). In addition, under NO atmosphere, the main mechanism of soot elimination did not change for Ce-based catalysts, while for trimetallic catalyst there is an increase in the removal capacity by the assisted and cooperative mechanism due to the presence of NO_2 and the intervention of the adsorbed

nitrate species on the catalyst, in a higher temperature operation window compared to Ce-containing catalysts.

Acknowledgements

MCR acknowledges the postdoctoral fellowship obtained from the University of Malaga. MCR, CH, MAL and LJA want to thank the financial support of CTQ 2017-87909R project. MCR also want to thank the University of Alicante for the financial support for the internship (INV19-07). JCMM and AGG gratefully acknowledge the financial support of Generalitat Valenciana (PROMETEO/2018/076 project) and the Spanish Ministry of Science, Innovation and Universities (PID2019-105542RB-I00 project) and the UE-FEDER funding. JCMM also acknowledges Spanish Ministry of Science, Innovation and Universities for the financial support through a FPU grant (FPU17/00603).

References

[1] A. Joshi, Review of vehicle engine efficiency and emissions, SAE Int. J. Adv. Curr. Pr. Mobil. 2 (2020) 2479–2507. doi:10.4271/2020-01-0352.

[2] A. Joshi, Review of vehicle engine efficiency and emissions, SAE Int. J. Adv. Curr. Pr. Mobil. 1 (2019) 734–761. doi:10.4271/2019-01-0314.

[3] M. Cortés-Reyes, C. Herrera, M.Á. Larrubia, L.J. Alemany, Hybrid technology for DeNOxing by LNT-SCR system for efficient diesel emission control: Influence of operation parameters in H_2O + CO_2 atmosphere, Catalysts. 10 (2020) 1–16. doi:10.3390/catal10020228.

[4] M. Abián, C. Martín, P. Nogueras, J. Sánchez-Valdepeñas, J. Rodríguez-Fernández, M. Lapuerta, M.U. Alzueta, Interaction of diesel engine soot with NO_2 and O_2 at diesel exhaust conditions. Effect of fuel and engine operation mode, Fuel. 212 (2018) 455–461. doi:10.1016/j.fuel.2017.10.025.

[5] F.C.P. Leach, M.S. Peckham, M.J. Hammond, Identifying NOx Hotspots in Transient Urban Driving of Two Diesel Buses and a Diesel Car, Atmosphere (Basel). 11 (2020) 355–373. doi:10.3390/atmos11040355.

[6] M. Sakota, T. Mori, K. Nemoto, T. Kogawa, Y. Kakizaki, Ag type PM oxidation catalyst with Nd added to increase contact property between PM an catalyst, SAE Int. J. Fuels Lubr. 11 (2018) 397–410. doi:10.4271/2018-01-0328.

[7] A. Joshi, T. V. Johnson, Gasoline Particulate Filters—a Review, Emiss. Control Sci. Technol. 4 (2018) 219–239. doi:10.1007/s40825-018-0101-y.

[8] R. Davis, G. Mandrusiak, T. Landenfeld, Development of the combustion system for General Motors' 3.6L DOHC 4V V6 engine with direct injection, SAE Int. J. Engines. 1 (2009) 85–100.

[9] C. Liu, R. Chen, F. Sera, A.M. Vicedo-Cabrera, Y. Guo, S. Tong, M.S.Z.S. Coelho, P.H.N. Saldiva, E. Lavigne, P. Matus, N. Valdes Ortega, S. Osorio Garcia, M. Pascal, M. Stafoggia, M. Scortichini, M. Hashizume, Y. Honda, M. Hurtado-Díaz, J. Cruz, B. Nunes, J.P. Teixeira, H. Kim, A. Tobias, C. Íñiguez, B. Forsberg, C. Åström, M.S. Ragettli, Y.-L. Guo, B.-Y. Chen, M.L. Bell, C.Y. Wright, N. Scovronick, R.M. Garland, A. Milojevic, J. Kyselý, A. Urban, H. Orru, E. Indermitte, J.J.K. Jaakkola, N.R.I. Ryti, K. Katsouyanni, A. Analitis, A. Zanobetti, J. Schwartz, J. Chen, T. Wu, A. Cohen, A. Gasparrini, H. Kan, Ambient Particulate Air Pollution and Daily Mortality in 652 Cities, N. Engl. J. Med. 381 (2019) 705–715. doi:10.1056/nejmoa1817364.

[10] T. Boger, D. Rose, P. Nicolin, N. Gunasekaran, T. Glasson, Oxidation of Soot (Printex® U) in Particulate Filters Operated on Gasoline Engines, Emiss. Control Sci. Technol. 1 (2015) 49–63. doi:10.1007/s40825-015-0011-1.

[11] S. Liu, X. Wu, D. Weng, R. Ran, Ceria-based catalysts for soot oxidation: A review, J. Rare Earths. 33 (2015) 567–590. doi:10.1016/S1002-0721(14)60457-9.

[12] S. Liu, X. Wu, W. Liu, W. Chen, R. Ran, M. Li, D. Weng, Soot oxidation over CeO_2 and Ag/CeO_2: Factors determining the catalyst activity and stability during reaction, J. Catal. 337 (2016) 188–198. doi:10.1016/j.jcat.2016.01.019.

[13] H. Wang, B. Jin, H. Wang, N. Ma, W. Liu, D. Weng, X. Wu, S. Liu, Study of Ag

promoted Fe_2O_3@CeO_2 as superior soot oxidation catalysts: The role of Fe_2O_3 crystal plane and tandem oxygen delivery, Appl. Catal. B Environ. 237 (2018) 251–262. doi:10.1016/j.apcatb.2018.05.093.

[14] X. Wang, B. Jin, R. Feng, W. Liu, D. Weng, X. Wu, S. Liu, A robust core-shell silver soot oxidation catalyst driven by Co_3O_4: Effect of tandem oxygen delivery and Co_3O_4-CeO_2 synergy, Appl. Catal. B Environ. 250 (2019) 132–142. doi:10.1016/j.apcatb.2019.03.019.

[15] J.C. Martínez-Munuera, M. Zoccoli, J. Giménez-Mañogil, A. García-García, Lattice oxygen activity in ceria-praseodymia mixed oxides for soot oxidation in catalysed Gasoline Particle Filters, Appl. Catal. B Environ. 245 (2019) 706–720. doi:10.1016/j.apcatb.2018.12.076.

[16] W.Y. Hernández, D. Lopez-Gonzalez, S. Ntais, C. Zhao, A. Boréave, P. Vernoux, Silver-modified manganite and ferrite perovskites for catalyzed gasoline particulate filters, Appl. Catal. B Environ. 226 (2018) 202–212. doi:10.1016/j.apcatb.2017.12.029.

[17] F. He, J. Chen, S. Liu, Z. Huang, G. Wei, G. Wang, Y. Cao, K. Zhao, $La_{1-x}Sr_xFeO_3$ perovskite-type oxides for chemical-looping steam methane reforming: Identification of the surface elements and redox cyclic performance, Int. J. Hydrogen Energy. 44 (2019) 10265–10276. doi:10.1016/j.ijhydene.2019.03.002.

[18] K. Li, H. Wang, Y. Wei, D. Yan, Transformation of methane into synthesis gas using the redox property of Ce-Fe mixed oxides: Effect of calcination temperature, Int. J. Hydrogen Energy. 36 (2011) 3471–3482. doi:10.1016/j.ijhydene.2010.12.038.

[19] K. Li, H. Wang, Y. Wei, D. Yan, Partial oxidation of methane to syngas with air by lattice oxygen transfer over ZrO_2-modified Ce-Fe mixed oxides, Chem. Eng. J. 173 (2011) 574–582. doi:10.1016/j.cej.2011.08.006.

[20] K. Zhao, Y. Shen, Z. Huang, F. He, G. Wei, A. Zheng, H. Li, Z. Zhao, Different oxidation routes for lattice oxygen recovery of double-perovskite type oxides $LaSrFeCoO_6$ as oxygen carriers for chemical looping steam methane reforming, J. Energy Chem. 26 (2017) 501–509. doi:10.1016/j.jechem.2016.11.016.

[21] M. Cortés-Reyes, M.C. Herrera, I.S. Pieta, M.A. Larrubia, L.J. Alemany, In situ TG-MS study of NOx and soot removal over LNT model catalysts, Appl. Catal. A Gen. 523 (2016) 193–199. doi:10.1016/j.apcata.2016.06.004.

[22] M. Cortés-Reyes, C. Herrera, M.Á. Larrubia, L.J. Alemany, Intrinsic reactivity analysis of soot removal in LNT-catalysts, Appl. Catal. B Environ. 193 (2016) 110–120. doi:10.1016/j.apcatb.2016.04.014.

[23] M. Cortés-Reyes, C. Herrera, M.Á. Larrubia, L.J. Alemany, Understanding of soot removal mechanism over DeNOx -catalysts as passive converters, Ind. Eng. Chem. Res. (2021). doi:10.1021/acs.iecr.0c05363.

[24] K. Klier, J. Novakova, P. Jiru, Exchange reactions of oxygen between oxygen molecules and solid oxides, J. Catal. 2 (1963) 479–484.

[25] E.M. Sadovskaya, A.S. Bobin, V. V. Skazka, Isotopic transient analysis of oxygen exchange over oxides, Chem. Eng. J. 348 (2018) 1025–1036.

doi:10.1016/j.cej.2018.05.027.

[26] M. Cortés-Reyes, C. Herrera, M.Á. Larrubia, L.J. Alemany, Advance in the scaling up of a hybrid catalyst for NSR-SCR coupled systems under H_2O + CO_2 atmosphere, Catal. Today. 356 (2020) 292–300. doi:10.1016/j.cattod.2019.05.010.

[27] M. V. Landau, M.L. Kaliya, A. Gutman, L.O. Kogan, M. Herskowitz, P.F. Van Den Oosterkamp, Oxidative conversion of LPG to olefins with mixed oxide catalysts: Surface chemistry and reactions network, Stud. Surf. Sci. Catal. 110 (1997) 315–326. doi:10.1016/s0167-2991(97)80992-5.

[28] C.Y. Yoo, H.J.M. Bouwmeester, Oxygen surface exchange kinetics of $SrTi_{1-x}Fe_xO_{3-\delta}$ mixed conducting oxides, Phys. Chem. Chem. Phys. 14 (2012) 11759–11765. doi:10.1039/c2cp41923h.

[29] S. Saher, J. Song, V. Vibhu, C. Nicollet, A. Flura, J.M. Bassat, H.J.M. Bouwmeester, Influence of annealing at intermediate temperature on oxygen transport kinetics of $Pr_2NiO_{4+\delta}$, J. Mater. Chem. A. 6 (2018) 8331–8339. doi:10.1039/c7ta08885j.

[30] C.Y. Yoo, B.A. Boukamp, H.J.M. Bouwmeester, Oxygen surface exchange kinetics on $PrBaCo_2O_{5+\delta}$, Solid State Ionics. 262 (2014) 668–671. doi:10.1016/j.ssi.2013.11.042.

[31] I. Atribak, A. Bueno-López, A. García-García, Uncatalysed and catalysed soot combustion under NOx+O_2: Real diesel versus model soots, Combust. Flame. 157 (2010) 2086–2094. doi:10.1016/j.combustflame.2010.04.018.

[32] N. Nejar, M. Makkee, M.J. Illán-Gómez, Catalytic removal of NOx and soot from diesel exhaust: Oxidation behaviour of carbon materials used as model soot, Appl. Catal. B Environ. 75 (2007) 11–16. doi:10.1016/j.apcatb.2007.03.009.

[33] B. Dernaika, D. Uner, A simplified approach to determine the activation energies of uncatalyzed and catalyzed combustion of soot, Appl. Catal. B Environ. 40 (2003) 219–229.

[34] L. Castoldi, R. Matarrese, L. Lietti, P. Forzatti, Intrinsic reactivity of alkaline and alkaline-earth metal oxide catalysts for oxidation of soot, Appl. Catal. B Environ. 90 (2009) 278–285. doi:10.1016/j.apcatb.2009.03.022.

[35] N. Guillén-Hurtado, A. García-García, A. Bueno-López, Isotopic study of ceria-catalyzed soot oxidation in the presence of NOx, J. Catal. 299 (2013) 181–187. doi:10.1016/j.jcat.2012.11.026.

[36] J.H. Lee, D.Y. Jo, J.W. Choung, C.H. Kim, H.C. Ham, K.Y. Lee, Roles of noble metals (M = Ag, Au, Pd, Pt and Rh) on CeO_2 in enhancing activity toward soot oxidation: Active oxygen species and DFT calculations, J. Hazard. Mater. 403 (2021) 124085. doi:10.1016/j.jhazmat.2020.124085.

[37] E. Poggio-Fraccari, B. Irigoyen, G. Baronetti, F. Mariño, Ce-Pr mixed oxides as active supports for Water-gas Shift reaction: Experimental and density functional theory characterization, Appl. Catal. A Gen. 485 (2014) 123–132. doi:10.1016/j.apcata.2014.07.040.

[38] A.M. D'Angelo, A.L. Chaffee, Correlations between Oxygen Uptake and

Vacancy Concentration in Pr-Doped CeO_2, ACS Omega. 2 (2017) 2544–2551. doi:10.1021/acsomega.7b00550.

[39] J. Deng, S. Li, L. Xiong, Y. Jiao, S. Yuan, J. Wang, Y. Chen, Preparation of nanostructured CeO_2-ZrO_2-based materials with stabilized surface area and their catalysis in soot oxidation, Appl. Surf. Sci. 505 (2020) 144301. doi:10.1016/j.apsusc.2019.144301.

[40] M. Ogura, R. Kimura, H. Ushiyama, F. Nikaido, K. Yamashita, T. Okubo, Carbonate-promoted catalytic activity of potassium cations for soot combustion by gaseous oxygen, ChemCatChem. 6 (2014) 479–484. doi:10.1002/cctc.201300736.

[41] Z. Shang, M. Sun, X. Che, W. Wang, L. Wang, X. Cao, W. Zhan, Y. Guo, Y. Guo, G. Lu, The existing states of potassium species in K-doped Co_3O_4 catalysts and their influence on the activities for NO and soot oxidation, Catal. Sci. Technol. 7 (2017) 4710–4719. doi:10.1039/c7cy01444a.

[42] R. Matarrese, L. Castoldi, L. Lietti, P. Forzatti, Soot combustion: Reactivity of alkaline and alkaline earth metal oxides in full contact with soot, Catal. Today. 136 (2008) 11–17. doi:10.1016/j.cattod.2008.03.022.

[43] Q. Li, Y. Xin, Z. Zhang, X. Cao, Electron donation mechanism of superior Cs-supported oxides for catalytic soot combustion, Chem. Eng. J. 337 (2018) 654–660. doi:10.1016/j.cej.2017.12.146.

[44] Q. Shen, G. Lu, C. Du, Y. Guo, Y. Wang, Y. Guo, X. Gong, Role and reduction of NOx in the catalytic combustion of soot over iron-ceria mixed oxide catalyst, Chem. Eng. J. 218 (2013) 164–172. doi:10.1016/j.cej.2012.12.010.

[45] N.D. Wasalathanthri, T.M. SantaMaria, D.A. Kriz, S.L. Dissanayake, C.H. Kuo, S. Biswas, S.L. Suib, Mesoporous manganese oxides for NO_2 assisted catalytic soot oxidation, Appl. Catal. B Environ. 201 (2017) 543–551. doi:10.1016/j.apcatb.2016.08.052.

[46] F. Jacquot, V. Logie, J.F. Brilhac, P. Gilot, Kinetics of the oxidation of carbon black by NO_2 Influence of the presence of water and oxygen, Carbon N. Y. 40 (2002) 335–343. doi:10.1016/S0008-6223(01)00103-8.

[47] A. Setiabudi, M. Makkee, J.A. Moulijn, The role of NO_2 and O_2 in the accelerated combustion of soot in diesel exhaust gases, Appl. Catal. B Environ. 50 (2004) 185–194. doi:10.1016/j.apcatb.2004.01.004.

[48] H. Zhang, S. Yuan, J.L. Wang, M. Gong, Y. Chen, Effects of contact model and NOx on soot oxidation activity over Pt/MnO_x-CeO_2 and the reaction mechanisms, Chem. Eng. J. 327 (2017) 1066–1076. doi:10.1016/j.cej.2017.06.013.

[49] V. Rico Pérez, A. Bueno-López, Catalytic regeneration of Diesel Particulate Filters: Comparison of Pt and CePr active phases, Chem. Eng. J. 279 (2015) 79–85. doi:10.1016/j.cej.2015.05.004.

[50] S.J. Jelles, R.R. Krul, M. Makkee, J.A. Moulijn, The influence of NOx on the oxidation of metal activated diesel soot, Catal. Today. 53 (1999) 623–630. doi:10.1016/S0920-5861(99)00150-9.

[51] M. Jeguirim, V. Tschamber, J.F. Brilhac, P. Ehrburger, Oxidation mechanism of carbon black by NO_2: Effect of water vapour, Fuel. 84 (2005) 1949–1956. doi:10.1016/j.fuel.2005.03.026.

[52] M. Jeguirim, V. Tschamber, P. Ehrburger, Catalytic effect of platinum on the kinetics of carbon oxidation by NO_2 and O_2, Appl. Catal. B Environ. 76 (2007) 235–240. doi:10.1016/j.apcatb.2007.05.029.

[53] M. Jeguirim, V. Tschamber, J.F. Brilhac, Kinetics of catalyzed and non-catalyzed soot oxidation with nitrogen dioxide under regeneration particle trap conditions, J. Chem. Technol. Biotechnol. 84 (2009) 770–776. doi:10.1002/jctb.2110.

[54] H. Zhang, C. Zhou, M.E. Galvez, P. Da Costa, Y. Chen, MnOx -CeO_2 mixed oxides as the catalyst for NO-assisted soot oxidation: The key role of NO adsorption/desorption on catalytic activity, Appl. Surf. Sci. 462 (2018) 678–684. doi:10.1016/j.apsusc.2018.08.186.

[55] R. Matarrese, L. Castoldi, L. Lietti, Reaction between soot and stored NOx over K-based LNT catalysts investigated by temperature programmed methods and labeling isotopic experiments, Catal. Today. 197 (2012) 228–235. doi:10.1016/j.cattod.2012.07.046.

[56] H. Tsukahara, T. Ishida, M. Mayumi, Gas-phase oxidation of nitric oxide: Chemical kinetics and rate constant, Nitric Oxide Biol. Chem. 3 (1999) 191–198. doi:10.1006/niox.1999.0232.

[57] B. Pereda-Ayo, U. De La Torre, M.P. González-Marcos, J.R. González-Velasco, Influence of ceria loading on the NOx storage and reduction performance of model Pt–Ba/Al_2O_3 NSR catalyst, Catal. Today. 241 (2015) 133–142. doi:10.1016/j.cattod.2014.03.044.

[58] L. Olsson, H. Persson, E. Fridell, M. Skoglundh, B. Andersson, A Kinetic Study of NO Oxidation and NOx Storage on Pt/Al_2O_3 and Pt/BaO/Al_2O_3, J. Phys. Chem. B. 105 (2001) 6895–6906. doi:10.1021/jp010324p.

[59] N. Bion, F. Epron, M. Moreno, F. Mariño, D. Duprez, Preferential oxidation of carbon monoxide in the presence of hydrogen (PROX) over noble metals and transition metal oxides: Advantages and drawbacks, Top. Catal. 51 (2008) 76–88. doi:10.1007/s11244-008-9116-x.

Figure Captions

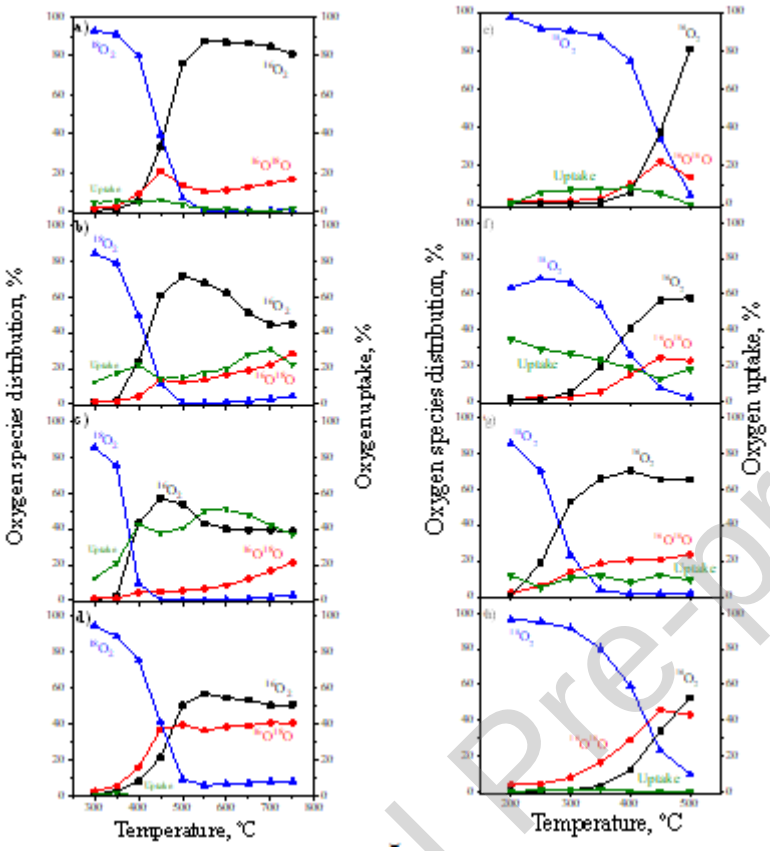

Figure 1. Gas phase distribution of each oxygen isotopologue ($^{16}O_2$, $^{16}O^{18}O$ and $^{18}O_2$) and oxygen uptake with respect to the inlet labeled oxygen at different temperatures under He flow over a) CeO_2, b) CePr-CP, c) CePr-DC and d) PtBaK and the same data after He pretreatment at 500ºC over e) CeO_2, f) CePr-CP, g) CePr-DC and h) PtBaK.

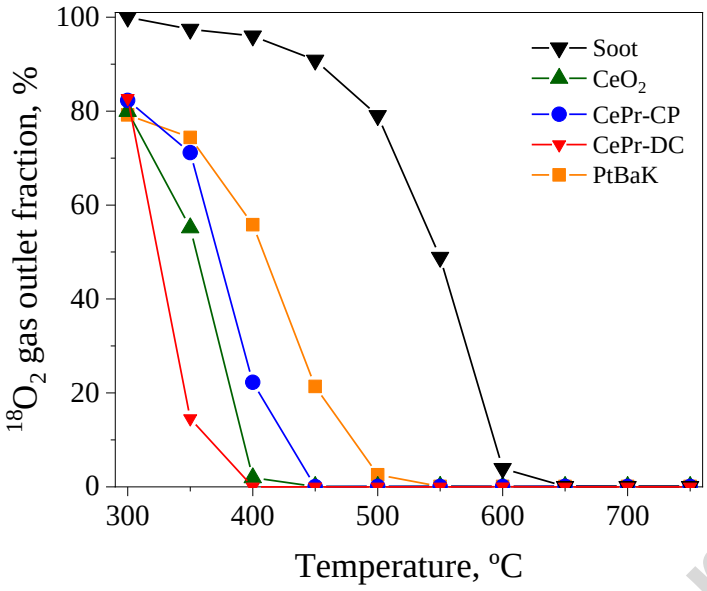

Figure 2. $^{18}O_2$ fraction (expressed as percentage) at the outlet during $^{18}O_2$ pulses over the samples with soot under He flow at different temperatures.

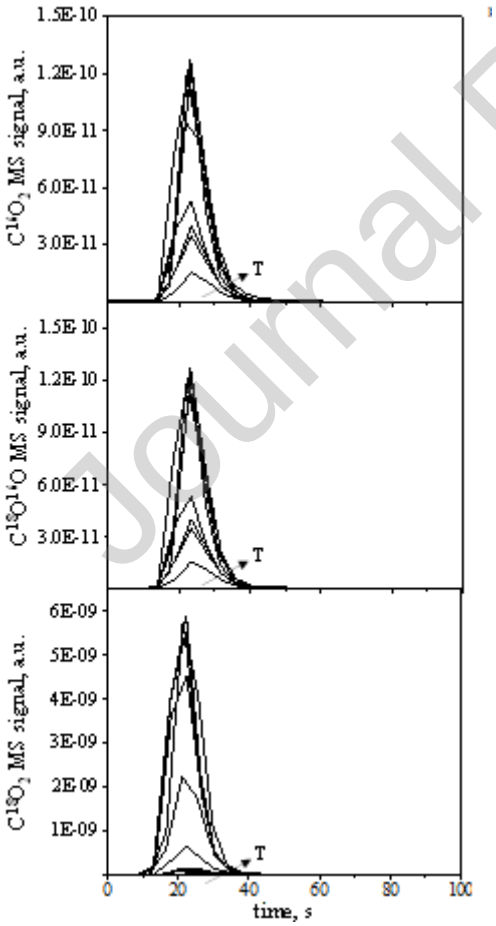

Figure 3. CO_2 isotopic distribution along a pulse of $^{18}O_2$ over bare-soot sample at different temperatures from 350 to 750ºC (50ºC steps).

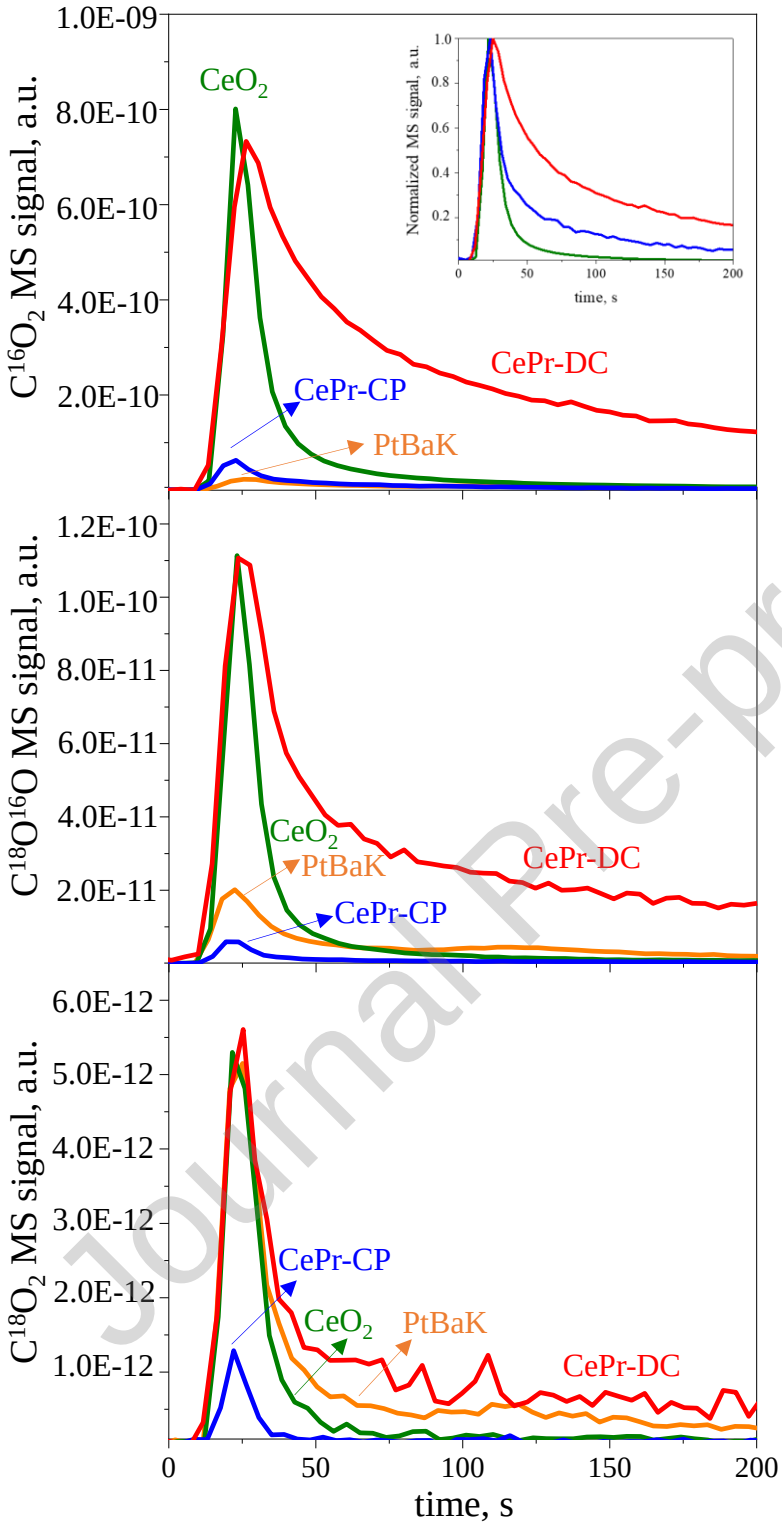

Figure 4. CO_2 isotopic distribution along a pulse of $^{18}O_2$ over CeO_2, CePr-CP, CePr-DC and PtBaK catalyst+soot mixtures at 350ºC under He atmosphere (inset normalized $C^{16}O_2$ MS signal for Ce-based materials).

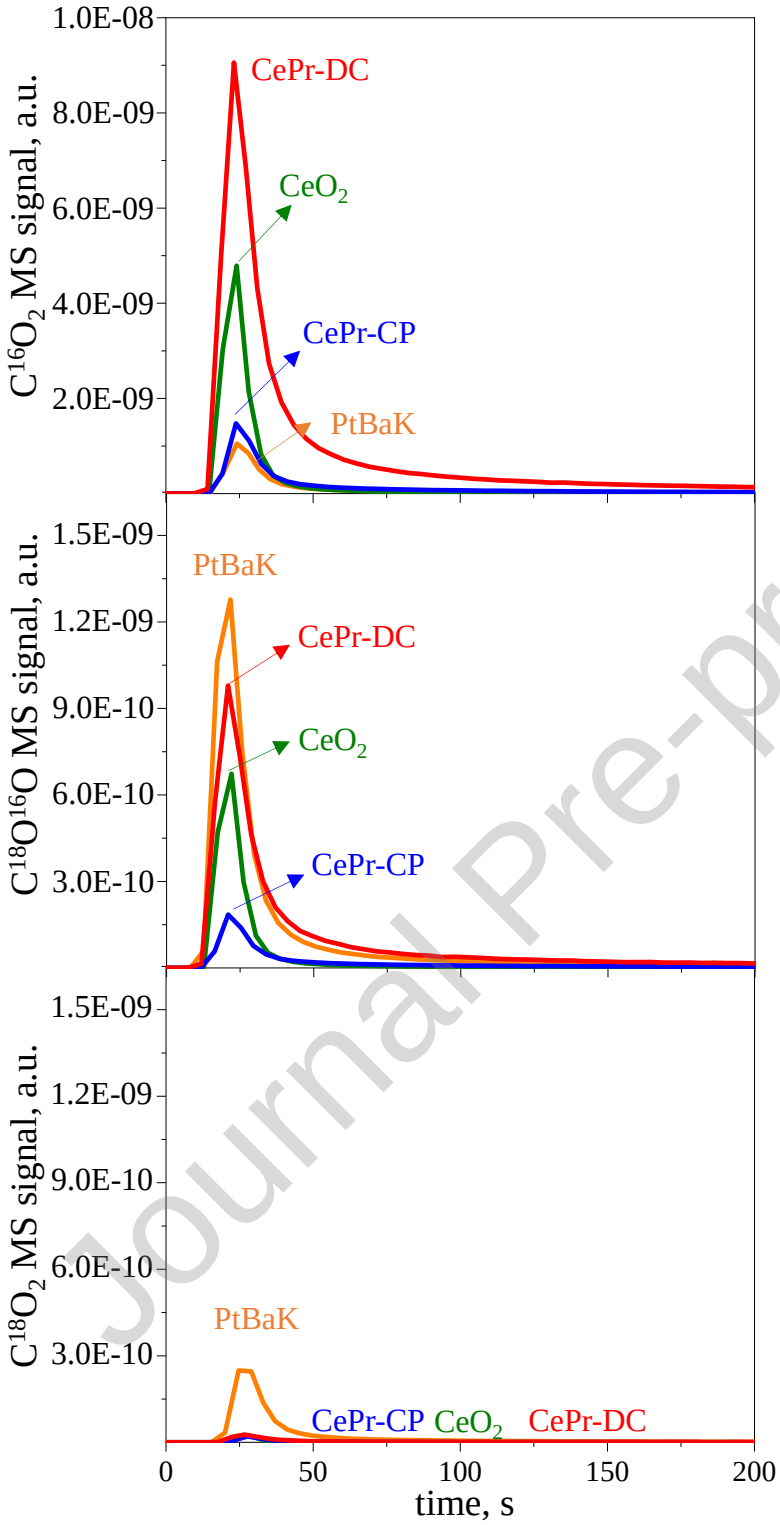

Figure 5. CO_2 isotopic distribution along a pulse of $^{18}O_2$ over CeO_2, CePr-CP, CePr-DC and PtBaK catalyst+soot mixtures at 500ºC under He atmosphere.

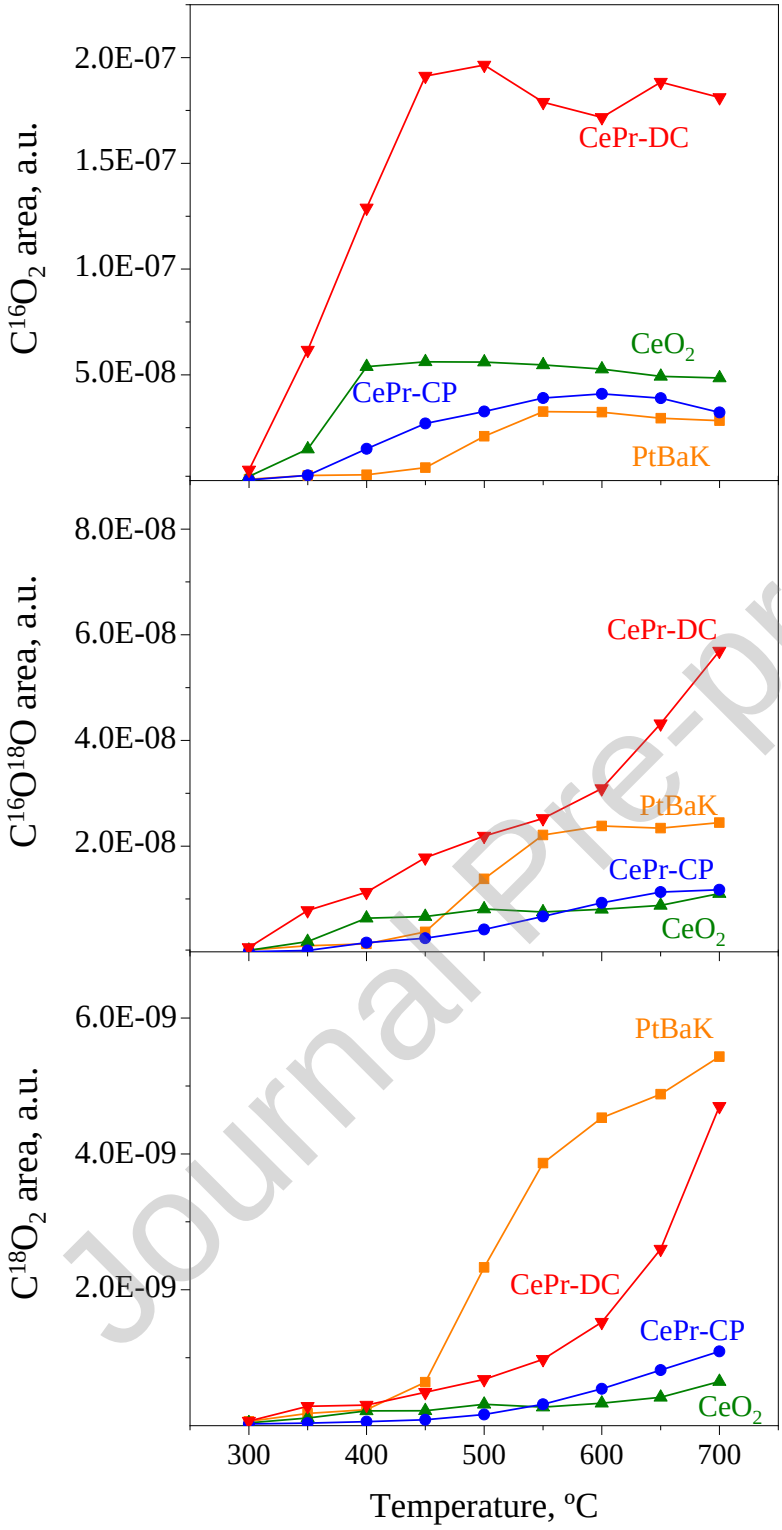

Figure 6. Area of each CO_2 isotopologue intensity along time of a pulse of $^{18}O_2$ over CeO_2, CePr-CP, CePr-DC and PtBaK catalyst+soot mixtures under He atmosphere at different temperatures.

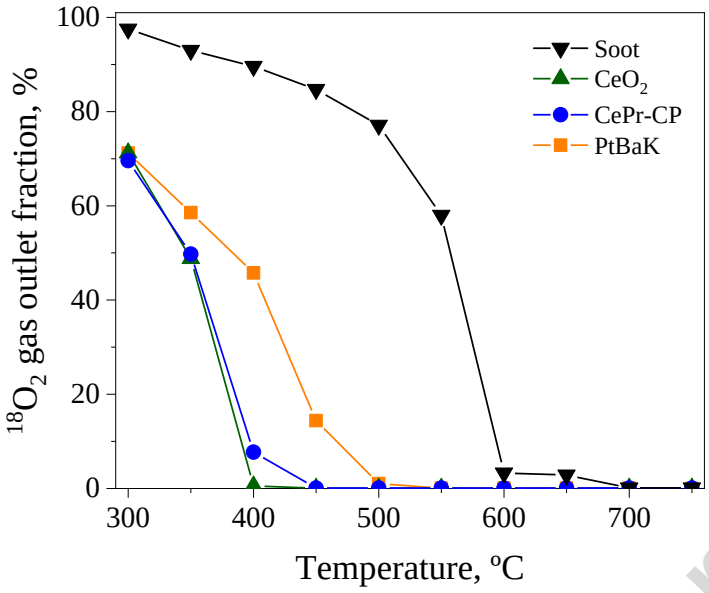

Figure 7. $^{18}O_2$ fraction (expressed as percentage) at the outlet during $^{18}O_2$ pulses over the samples with soot under 1%NO in He flow at different temperatures.

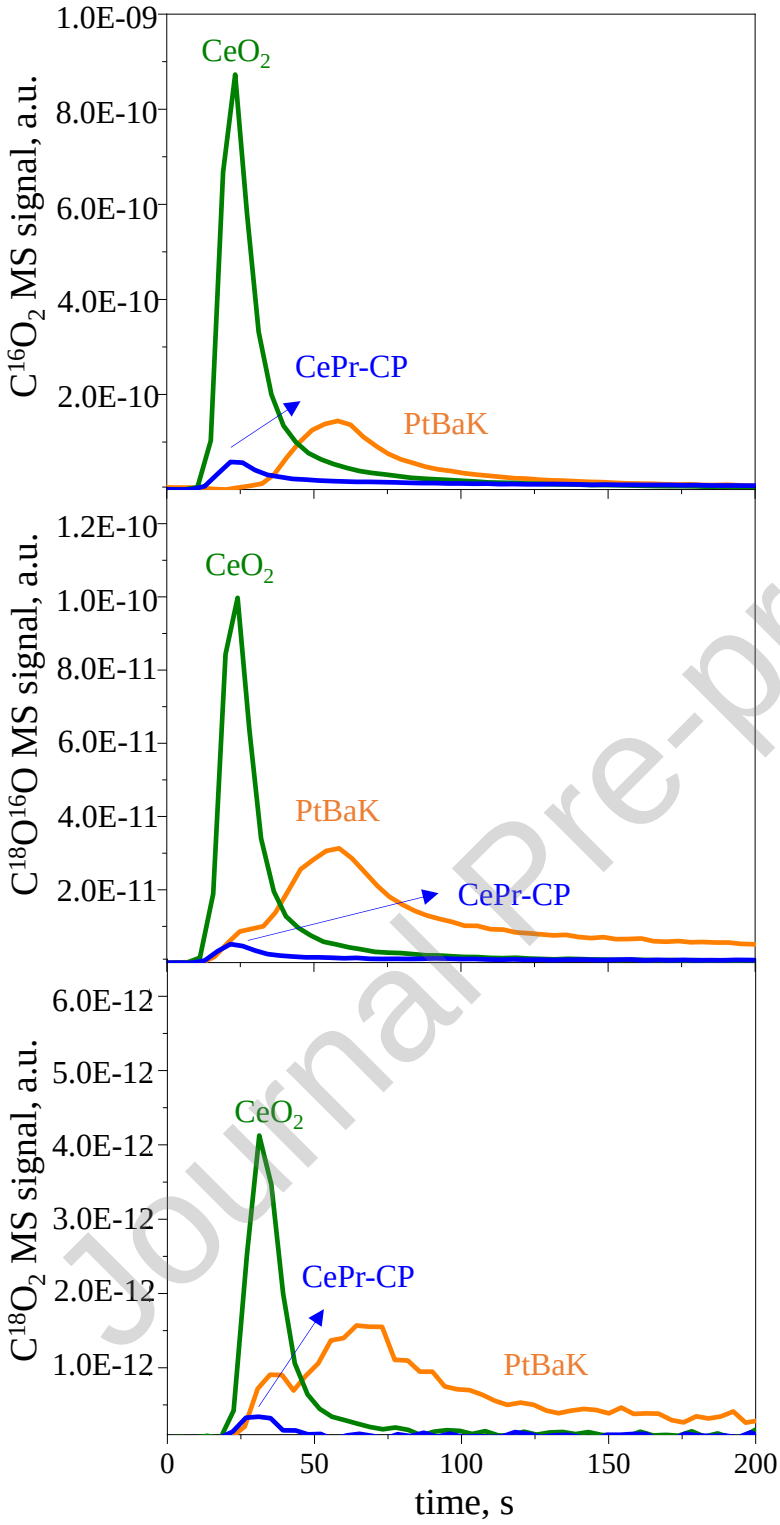

Figure 8. CO_2 isotopic distribution along a pulse of $^{18}O_2$ over CeO_2, CePr-CP, CePr-DC and PtBaK catalyst+soot mixtures at 350ºC under 1%NO in He atmosphere.

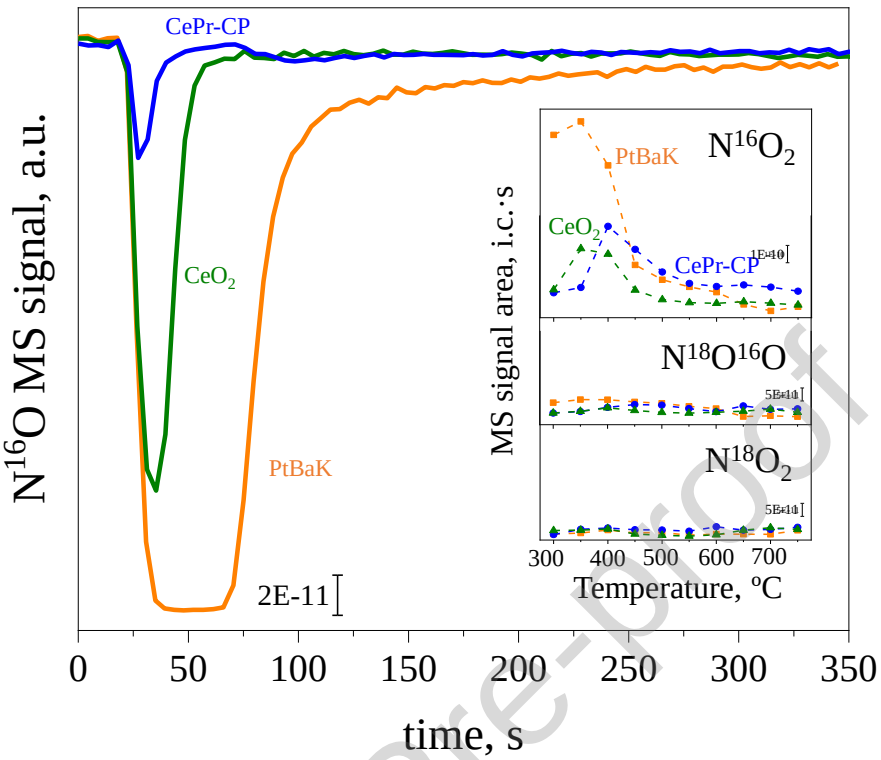

Figure 9. Unlabeled NO MS signal according to time during a pulse of $^{18}O_2$ at 350ºC (inset of NO_2 isotopologues area along the pulse as a function of temperature).

CRediT authorship contribution statement

Marina Cortés Reyes: Methodology, Investigation, Conceptualization, Writing-review; Juan Carlos Martínez-Munuera: Methodology, Investigation; Concepción Herrera: Investigation, Writing - review ; M. Ángeles Larrubia: Investigation, Writing - review ; Luis J. Alemany: Conceptualization, Resources, Writing - review & editing, Supervision; Avelina García-García: Conceptualization, Resources, Writing - review & editing, Supervision;

Declaration of Competing **Interest**

☒ The authors declare that they have no known competing financial interests or personal relationships that could have appeared to influence the work reported in this paper.

☐The authors declare the following financial interests/personal relationships which may be considered as potential competing interests:

Highlights

- For CeO_2 catalysts the $^{18}O_2/^{16}O_2$ exchange prevails and Pr increases oxygen uptake
- PtBaK promotes single-atom exchange being $^{18}O^{16}O$ the main detected species
- Soot removal mechanism depends on oxygen species (O_I, O_{II} or O_{III} type) mobility
- CePr mixed oxides are able to remove soot at low temperature under inert conditions
- DPNR catalyst is more efficient in the presence of NO due to nitrate intervention